12-19-2017

Changes in Enzyme Structural Dynamics Studied by Hydrogen Exchange-Mass Spectrometry: Ligand Binding Effects or Catalytically Relevant Motions?

Courtney S Fast

Siavash Vahidi

Lars Konermann

Changes in Enzyme Structural Dynamics Studied by Hydrogen Exchange-Mass Spectrometry: Ligand Binding Effects or Catalytically Relevant Motions?

Courtney S. Fast, Siavash Vahidi, and Lars Konermann*

Department of Chemistry, The University of Western Ontario, London, Ontario, N6A 5B7, Canada

* To whom correspondence should be addressed. Telephone: (519) 661-2111 ext. 86313.

Email: konerman@uwo.ca

ABSTRACT: It is believed that enzyme catalysis is facilitated by conformational dynamics of the protein scaffold that surrounds the active site. Yet, the exact nature of catalytically relevant protein motions remains largely unknown. Hydrogen/deuterium exchange (HDX) mass spectrometry (MS) reports on backbone H-bond fluctuations. HDX/MS thus represents a promising avenue for probing the relationship between enzyme dynamics and catalysis. A seemingly straightforward strategy for such studies involves comparative measurements during substrate turnover and in the resting state. We examined the feasibility of this approach using rabbit muscle pyruvate kinase (*r*M1-PK) which catalyzes the conversion of phosphoenolpyruvate and Mg-ADP to pyruvate and Mg-ATP. HDX/MS revealed that catalytically active *r*M1-PK undergoes significant rigidification in the active site. This finding is counterintuitive, considering the purported correlation between dynamics and catalysis. Interestingly, virtually the same rigidification was seen upon exposing *r*M1-PK to substrates or products in the absence of turnover. These data imply that the active site dynamics during turnover are dominated by protein-ligand binding interactions. These interactions stabilize H-bonds in the vicinity of the active site, thereby masking subtle dynamic features that might be uniquely associated with catalysis. Our data uncover an inherent problem with side-by-side turnover/resting state measurements, i.e., the difficulty to design a suitable reference state against which the working enzyme can be compared. Comparative HDX/MS experiments on enzyme dynamics should therefore be interpreted with caution.

The catalytic power of enzymes is remarkable, with rate enhancements up to nineteen orders of magnitude.[1] This acceleration results from lowered activation barriers, often in conjunction with the breakdown of reactions into multi-step sequences.[2, 3] A central aspect of enzyme catalysis is the stabilization of transition states in the active site by H-bonds, the judicious positioning of proton donors/acceptors, transiently formed covalent linkages, and the exclusion of water.[1, 4] Metal cofactors can provide electrostatic contacts, Lewis acid/base interactions, and electron shuttling.[5, 6]

Like other proteins, enzymes undergo conformational dynamics, with motions that range from picosecond side chain fluctuations to sub-second domain movements and unfolding/refolding transitions.[7-9] Enzyme dynamics are considered to be a key prerequisite for catalysis.[3, 10-18] This view is reinforced by X-ray structures that show large alterations upon substrate or inhibitor binding, compared to the catalytically inactive resting state.[19-23] These crystallographically detectable changes typically lead from an unbound "open" conformation to a "closed" state where the substrate is occluded from the solvent while catalysis takes place. Subsequent product release requires an opening event, before the next turnover cycle commences.[24] Steady-state catalysis must therefore be accompanied by incessant opening/closing transitions. Structural fluctuations may also mediate molecular contacts that are required for bond formation or dissociation.[3, 10-18] The exact role of conformational dynamics for binding, release, and for the reshuffling of chemical bonds nonetheless remains controversial.[25-27]

A seemingly straightforward approach for deciphering the relationship between dynamics and catalysis is to compare the properties of working enzymes with those of the resting state. Experiments on dihydrofolate reductase suggest that the presence of substrate guides conformational motions along a specific reaction path.[28] The internal dynamics of chymotrypsin were reported to be enhanced during catalysis.[13] In contrast, the dynamics of thermolysin were indistinguishable during catalysis and in the resting state,[29] supporting the view that catalytically

relevant motions are “intrinsic” and do not strongly depend on the presence of substrate (as previously suggested for the nano- to millisecond dynamics of adenylate kinase).[30] Thus, a consistent picture has not emerged yet.

Active/resting state comparative experiments are complicated by the fact that some changes caused by substrates, intermediates, or products may not be directly related to catalysis. Ligand binding generally affects the protein energy landscape, thereby altering conformational preferences.[31] Ligand-bound proteins are usually less dynamic than the corresponding apo-states. This effect arises from the cooperative stabilization of intramolecular linkages by intermolecular contacts.[32-45] However, local or global destabilization can take place as well.[46-49] It is therefore not obvious if altered enzyme dynamics during turnover are the result of catalytically relevant motions, or if they arise from rather trivial ligand binding effects. For deciphering these different scenarios it is necessary to supplement active/resting state comparisons with experiments that involve binding *without* turnover (e.g. by providing only one of two required substrates, or by exposing the enzyme to substrate mimics). It appears that the need for such control experiments has been under-appreciated in the literature.

Pyruvate kinase catalyzes the glycolytic conversion of phosphoenolpyruvate (PEP) and Mg-ADP to pyruvate and Mg-ATP. Four mammalian variants have been identified.[50, 51] The L and R isoforms are found in liver and red blood cells, respectively. M2 is expressed in embryonic tissues and during tumorigenesis,[51-54] and it is allosterically regulated by fructose-1,6-bisphosphate (FBP).[55, 56] The M1 isoform is found in adult brain tissue and skeletal muscle; it does not bind FBP and is constitutively active under typical conditions.[50, 53, 56]

Rabbit skeletal muscle pyruvate kinase (*r*M1-PK) represents the most extensively studied form of M1.[22, 57-62] The 232 kDa protein has a homo-tetrameric structure. Each subunit comprises four domains, termed N, A, B, and C. The active sites (one per subunit) are located in clefts

between domains B and A (Figure 1).[22] Each active site contains one K^+ and one Mg^{2+} ion, for a total of two Mg^{2+} once Mg-ADP or Mg-ATP are bound.[63] The reaction (Figure 1b) involves binding of PEP and Mg-ADP, followed by phosphate transfer from PEP to Mg-ADP. Mg-ATP then departs, leaving behind pyruvate in the enolate form which has its two negative charges coordinated by Mg^{2+}. Subsequent ketonization of the enolate produces pyruvate and supplies much of the driving force for the reaction.[22, 55] X-ray structures provide insights into some of the events associated with catalysis.[22] Crystals were grown in the presence of Mg-ATP and oxalate. The latter mimics the enolate form of pyruvate.[64] The data showed three subunit conformations, a fully closed Mg-ATP/oxalate-bound state, a semi-open Mg-ATP/oxalate-bound structure, and an oxalate-bound open conformation (Figure 1c-e). The open/closed transition involves a 41° rotation of domain B relative to A. These structures[22] suggest that each turnover event is accompanied by large-scale opening/closing events of the active site, making *r*M1-PK an ideal model system for probing the relationship between dynamics and catalysis.

Nuclear magnetic resonance (NMR) spin relaxation experiments are a well-established tool for probing enzyme dynamics,[28, 30, 65] but the application of this technique to systems as large as *r*M1-PK is difficult. Also, NMR requires proteins to be stable at high concentration (0.1 to 1 mM) for hours or days. Hydrogen/deuterium exchange (HDX) mass spectrometry (MS) represents an alternative bioanalytical approach[13, 16, 29] that overcomes these limitations.[35, 45, 66-68] The technique reports on conformational dynamics by monitoring the stability of backbone amide H-bonds. Segments that are tightly folded undergo slow deuteration, while flexible and/or disordered regions exhibit much faster HDX.[69] HDX/MS provides an integrative view of fluctuations that take place on time scales of microseconds to seconds.[70] This approach has been widely used for probing enzyme dynamics, with applications ranging from mechanistic investigations[13, 29, 71, 72] to structure-activity relationships in the context of drug discovery.[73, 74] Also, HDX/MS has been

applied to M1 and other pyruvate kinase variants for probing allosteric regulation,[57, 75, 76] but not for examining the relationship between dynamics and catalysis.

The current work addresses the question whether working/resting state HDX/MS comparisons can uncover catalytically relevant enzyme motions. The HDX behavior of *r*M1-PK was probed during catalysis, in the resting state, and in the presence/absence of various ligands that mimic different stages of the turnover process. Our data reveal major alterations in the extent and spatial distribution of conformational fluctuations during turnover. However, these changes are dominated by ligand binding effects. Catalytically relevant motions that take place during turnover are masked by ligand-induced rigidification of the active sites. These results uncover fundamental challenges related to the interpretation of active/resting state comparative data.

Methods

*r*M1-PK was purchased from Sigma Aldrich. Detailed biochemical and MS-based analyses were conducted to verify the enzymatic activity and structural integrity of the protein samples (see SI for a detailed summary of Materials, Methods, and Protein Characterization). Unless noted otherwise, all experiments were performed in 50 mM Tris buffer, 100 mM KCl, and 8 mM $MgCl_2$ at pH 7.5 with a *r*M1-PK concentration of 0.125 μM (as tetramer). Different types of samples were tested. (i) In the absence of any other solutes, the aforementioned solution conditions provide the *r*M1-PK resting state. (ii) Working state experiments were conducted in the presence of 10 mM ADP and 7.5 mM PEP. The time period during which the enzyme maintains turnover can be estimated as (limiting substrate concentration)/(k_{cat} × active site concentration) = 7500 μM / (274 s^{-1} × 0.5 μM) ≈ 1 min. Keeping the enzyme in the working state for a longer time interval would

require higher substrate concentrations. Unfortunately, this was not possible due to ADP-mediated signal suppression of peptic peptides. (iii) Substrate binding experiments were performed in the presence of either 2 mM ADP or PEP. (iv) Pseudo-product binding experiments were performed with 5 mM ATP and/or 1 mM potassium oxalate. (v) Metal-depleted *r*M1-PK (produced by dialysis in the presence of EDTA) was studied in 50 mM Tris buffer; for K^+ and Mg^{2+} binding experiments the solutions were supplemented with 100 mM KCl or 8 mM $MgCl_2$, respectively. HDX was carried out in 90% D_2O at pD 7.5. The samples were analyzed on a nanoACQUITY UPLC equipped with HDX technology (Waters, Milford, MA). The LC outflow was directed to a Waters Synapt Q-TOF G2 ESI mass spectrometer. DynamX 3.0 was used for data analysis. Error bars represent standard deviations derived from three independent sets of experiments for each condition.

Results and Discussion

Conformational Dynamics During Catalysis. HDX/MS measurements on *r*M1-PK were carried out under various conditions. In all cases the K^+/Mg^{2+}-saturated resting state served as reference. We will initially discuss data for the working enzyme, obtained by monitoring deuterium incorporation into *r*M1-PK while the PEP + Mg-ADP $\rightarrow$ pyruvate + Mg-ATP conversion proceeded in solution. As noted in the Methods section, these turnover conditions could be maintained for one minute. HDX/MS yielded information on the deuteration behavior of peptides throughout the protein, but we will pay particular attention to three segments located in the active site (Figure 2a). Segment 110-123 binds K^+ and is in contact with the phosphate groups of Mg-ADP or Mg-ATP. Also, this region forms part of the hinge that allows for the movement of domain B relative to A during turnover. Segment 292-298 accommodates the non-nucleotide

Mg^{2+}, and it interacts with PEP and pyruvate (or oxalate in the crystal structure).[22, 55] Segment 365-374 interacts with the adenine moiety of Mg-ADP or Mg-ATP.

As an example, mass spectra for segment 365-374 in the resting state and under working conditions for t = 1 min are shown in Figure 2b and 2c. It is readily apparent that working conditions caused significantly reduced deuteration compared to the resting state. After normalization (see SI Methods), it was found that the deuteration difference for segment 365-374 at t = 1 min was 36%. Even for measurements taken after 6 s this segment already showed a deuteration difference of 18% (Figure 3c). Reduced HDX levels under working conditions were also observed for the active site peptides 110-123 and 292-297, albeit the differences were not as dramatic as for 365-374 (Figure 3a, b). For visualizing the HDX response across the entire protein the measured deuteration differences for t = 1 min were mapped to the crystal structure (Figure 4a). All color maps use a scale where blue indicates regions that are less dynamic (i.e. with less deuteration) than the resting state; segments shown in red are more dynamic, as indicated in the legend of Figure 4. Figure 4a reinforces the finding that peptides in the vicinity of the active site exhibited strongly reduced deuteration under working conditions. Slightly elevated HDX levels (~10%) were apparent in some domain B segments, while the N and C domains were hardly affected (Figure S6).

The reduced deuteration in the *r*M1-PK active site during the 1 min catalytic activity window is unexpected. Studies on other enzymes under turnover conditions found that structural dynamics were enhanced,[13] altered,[28] or unchanged.[29, 30] To the best of our knowledge a turnover-induced rigidification of the H-bonding network, as observed here for *r*M1-PK, has not been reported previously. From the measured k_{cat} it can be estimated that each subunit undergoes 274 s^{-1} × 60 s ≈ 16,000 turnover events during the experimental time window, which must be accompanied by at least as many active site opening/closing transitions (Figure 1c, e). One might

have expected that these large-scale movements contribute to enhanced dynamics in the active site or in the domain B/A hinge region during turnover. However, this expectation is not confirmed by the experimental data. Several earlier studies indicated that reduced conformational dynamics generally suppress catalytic efficiency.[16, 17, 77] The rigidification seen here for catalytically active *r*M1-PK thus seems counterintuitive, considering the widely accepted paradigm that conformational fluctuations are a prerequisite for enzyme function.[3, 10-18] The observed behavior prompted us to examine the response of the protein to the presence or absence of a range of mechanistically relevant ligands, as described below (see the following three sections).

For time points beyond the 1 min range, where most of the substrate has been converted, the deuteration behavior of segment 110-123 approached that of the resting state (Figure 3a). In contrast, HDX differences of 292-298 and 365-374 persisted for longer times (Figure 3b, c). The behavior of these two segments likely reflects the phenomenon of ATP inhibition, where Mg-ATP is in excess and residual PEP remains bound in the *r*M1-PK active site.[78]

Substrate Binding. Catalytic turnover by *r*M1-PK requires the presence of both PEP and Mg-ADP (Figure 1b). By adding just one of these compounds it is possible to examine changes in enzyme dynamics in response to substrate *binding*, as opposed to turnover. HDX/MS profiles measured upon addition of PEP showed markedly reduced deuteration in a number of peptides, particularly 292-298 and 365-374 in the active site (Figure 3e, 3f). The magnitude and spatial distribution of the PEP-induced changes resembled the effects seen under turnover conditions (Figure 4a, 4b). The addition of Mg-ADP (without PEP) only caused relatively minor changes in the deuteration behavior relative to the resting state (Figure 3d-f, Figure 4c).

Pseudo-Product Binding. We also aimed to characterize the response of *r*M1-PK to reaction products in the solution. The canonical products are pyruvate and Mg-ATP. However, the binding affinity of *r*M1-PK to pyruvate in the absence of Mg-ATP is quite low, such that unreasonably high concentrations (> 10 mM) would be required to achieve significant binding levels.[22] The tendency of pyruvate to dimerize under such conditions would cause additional complications.[79] Following earlier crystallographic studies on *r*M1-PK[22] we thus exposed the protein to oxalate, which has a much higher binding affinity than pyruvate. Oxalate mimics the enolate that is transiently formed in the active site as obligatory intermediate during PEP → pyruvate conversion (Figure 1b).[64]

Exposure to Mg-ATP caused only minor changes in the deuteration behavior of *r*M1-PK relative to the resting state. In contrast, the presence of oxalate significantly lowered deuteration levels in the active site. Even more pronounced effects were seen when both species were present simultaneously, demonstrating that oxalate and Mg-ATP stabilize the active site H-bond network in a synergistic fashion (Figure 3g-i). The HDX difference maps generated for the oxalate and oxalate/Mg-ATP-bound protein (Figure 4d, f) closely resemble that of the working enzyme (Figure 4a). In all three cases, the blue-colored regions in domain A reflect rigidification of the H-bond network in the vicinity of the active site (Figure 4a, d, f).

Metal Cofactor Effects. To further characterize the response of *r*M1-PK to intermolecular contacts we examined the consequences of K^+ and Mg^{2+} depletion, being aware of the fact that such conditions are not necessarily relevant in a physiological context. K^+/Mg^{2+}depletion induced dramatically increased deuteration in the active site where the metal binding sites are located. Other protein regions were affected to a much lesser extent (Figure 3j-l, Figure 4g). Upon supplementing the metal-depleted protein with K^+ or Mg^{2+} it was found that the latter was more

effective in terms of restoring the stability of the H-bonding network (Figure 4h, i). This behavior is consistent with the fact that divalent ions usually interact more strongly with proteins than monovalent species.[5] In *r*M1-PK the non-nucleotide Mg^{2+} is tightly chelated by Glu273 and Asp296, while K^+ binds Asp113 and interacts with two side chain and one main chain oxygen.[22]

HDX kinetics can be modulated to some extent by electrostatic effects.[80-82] For example, positive charge density on a protein might favor the local accumulation of OD^- catalyst (thereby enhancing HDX rates), whereas the opposite would be expected for negative charge density. The observation that metal ion binding *decreases* HDX levels in *r*M1-PK (and in other proteins)[83, 84] demonstrates that such electrostatic effects are minor.[85] This is particularly true for experiments that use relatively high ionic strength (e.g. ~150 mM in this work) which shields charge-charge interactions.[32, 81] These considerations reinforce the view[35, 45, 66-68] that HDX differences for the various conditions of Figure 3 arise from alterations in H-bond dynamics.[35, 45, 66-68]

Ligand-Induced Active Site Stabilization vs. Catalytically Relevant Motions. The HDX/MS experiments described above reveal that H-bond fluctuations of *r*M1-PK are strongly affected by the presence of ligands. Binding to PEP, oxalate, or oxalate/Mg-ATP causes significant stabilization of the active site. This behavior suggests that the active site exhibits induced-fit behavior, where pliable elements fold around the ligand. Such scenarios have previously been documented for many other protein-ligand interactions.[86, 87] In all those cases intermolecular contacts trigger conformational changes that stabilize the protein scaffold surrounding the ligand binding site.[32-45] The high sensitivity of the active site for ligand-induced stabilization is further emphasized by the finding that Mg^{2+} removal dramatically increases the extent of deuteration, implying that metal binding is subject to induced fit behavior as well.

Close inspection of the Figure 4b-f color maps reveals red hues in domain B, indicating that this region which is somewhat remote from the active site shows a slight destabilization in the presence of catalytically relevant ligands. This behavior is consistent with earlier reports that ligand binding can cause stabilization as well as destabilization in different protein regions.[46-49]

Strikingly, the HDX patterns observed upon binding of PEP, oxalate, or oxalate/Mg-ATP under conditions that preclude substrate turnover (Figures 4b, d, f) are very similar to the HDX pattern observed under working conditions (Figure 4a). From this finding we conclude that changes in the *r*M1-PK H-bonding network seen under working conditions primarily reflect the protein response to *binding* interactions, rather than the occurrence of catalytically relevant enzyme motions. In other words, H-bond stabilization during catalysis arises from the fact that the protein cycles through various ligand-bound states under working conditions (E·PEP·Mg-ADP, E·enolate·Mg-ATP, E·enolate, see Figure 1b). Accumulation of the enolate-bound species under working conditions has been verified experimentally.[88] In addition, a significant a steady-state population of E·PEP en route towards E·PEP·Mg-ADP cannot be ruled out. Our observations imply that interactions with PEP and enolate are primarily responsible for the rigidification during catalysis, while the presence of Mg-ADP and Mg-ATP has less pronounced effects on H-bond stability.

Very minor differences are apparent between the working state HDX map (Figure 4a) and the data obtained for the PEP, oxalate, and oxalate/Mg-ATP-bound states (Figure 4b, d, f). However, attempts to interpret these small effects as a signature of unique catalytic motions would be tenuous, keeping in mind that no ligand-bound state will represent a perfect comparator for the working enzyme.

We do not dispute that conformational dynamics play a role for the *r*M1-PK catalytic mechanism, as implied by the closed/open crystal structures of Figure 1c and 1e.[22] In addition to

these large domain movements, small-scale fluctuations may facilitate the chemical conversion steps taking place during catalysis.[17] However, the HDX/MS data fail to uncover any conformational events that are uniquely linked to catalysis. Rather, the deuteration kinetics are dominated by ligand-induced stabilization that is encountered regardless whether turnover takes place or not. Any efforts to specifically identify catalytically relevant motions within the wide spectrum of *r*M1-PK dynamics[8, 9] are stymied by the masking contributions of rather mundane ligand binding effects. Clearly, binding-induced stabilization is associated with *r*M1-PK catalysis, but this stabilization does not represent a *unique* feature of the catalytically active protein because the same stabilization effects can be induced in the absence of turnover.

Conclusions

The question addressed in this work is whether working/resting state comparative HDX/MS measurements can provide direct information on the nature of catalytically relevant enzyme motions. The idea behind such experiments seems straightforward. The concept is analogous to trying to decipher the function of an industrial assembly line by examining a factory on a Sunday when the machinery is on standby, followed by a comparative inspection during the week when raw material is converted to product. Within this simple analogy it will undoubtedly be possible to uncover how motions of individual machine parts contribute to the overall turnover process.

In the case of enzymes, the situation is more complex. All proteins are subject to incessant thermal motions as they cycle through their Boltzmann-allowed conformational space.[8, 9] Some of these fluctuations may be catalytically relevant, while others represent unproductive "noise". Catalytically relevant motions may be facilitated by the presence of substrate in the active site,[13, 28] while others are intrinsic.[29, 30] During enzymatic turnover there will be a certain fraction of time

during which the active site is bound to substrates, intermediates, or products; these bound conditions will alternate with periods where the active site is vacant and primed for the binding of new substrates that would initiate the next turnover cycle. When aiming to design comparative measurements for identifying motions that are uniquely linked to catalysis, it may be impossible to select a suitable state against which the working enzyme can be appraised. The resting state is not appropriate because it lacks pertinent ligand-protein interactions. On the other extreme, binding of catalytically relevant species to the active site without turnover (as in Figure 4b-f) results in ligand-protein interactions that are much more permanent than those encountered during turnover. Neither condition provides a proper comparison base, which is why HDX difference maps are unlikely to reveal dynamic features that are uniquely linked to catalysis. Other enzymes may be less prone to binding-induced alterations than *r*M1-PK,[29, 30] but this does not imply that differences seen in working/resting state comparisons for those other systems will necessarily pinpoint catalytically relevant motions.

Overall, the current work demonstrates that efforts to elucidate linkages between enzyme dynamics and catalysis via comparative measurements should be treated with caution, although there is no shortage of such experiments in the literature. This conclusion is likely not limited to HDX/MS but also extends to other bioanalytical tools. In the case of *r*M1-PK we observed dramatic changes in the extent of conformational dynamics during catalysis. These changes are not unique to catalysis, but they arise from binding interactions that can also be implemented in the absence of turnover. The dominance of binding-related effects over catalytically relevant motions is also supported by recent kinase NMR spin relaxation data.[89] Likewise, binding-related stabilization[32-45] (or destabilization)[46-49] phenomena have been reported for many non-enzymatic proteins. Based on currently available data it appears that the magnitude of such binding-

associated dynamic changes dwarfs subtle conformational events that might be uniquely linked to enzymatic turnover.

Acknowledgements. We thank Stanley D. Dunn for valuable suggestions and feedback during the early stages of this project.

Funding. Financial support was provided by the Natural Sciences and Engineering Research Council of Canada (Discovery Grant 217080-2013).

Supporting Information. Additional experimental details and data as noted in the text.

References

(1) Wolfenden, R.; Snider, M. J. *Accounts Chem. Res.* **2001**, *34*, 938-945.
(2) Cleland, W. W.; Northrop, D. B. *Meth. Enzymol.* **1999**, *308*, 3-27.
(3) Kerns, S. J.; Agafonov, R. V.; Cho, Y. J.; Pontiggia, F.; Otten, R.; Pachov, D. V.; Kutter, S.; Phung, L. A.; Murphy, P. N.; Thai, V.; Alber, T.; Hagan, M. F.; Kern, D. *Nat. Struct. Mol. Biol.* **2015**, *22*, 124-131.
(4) Vocadlo, D. J.; Davies, G. J.; Laine, R.; Withers, S. G. *Nature* **2001**, *412*, 835-839.
(5) Yu, F. T.; Cangelosi, V. M.; Zastrow, M. L.; Tegoni, M.; Plegaria, J. S.; Tebo, A. G.; Mocny, C. S.; Ruckthong, L.; Qayyum, H.; Pecoraro, V. L. *Chem. Rev.* **2014**, *114*, 3495-3578.
(6) Valdez, C. E.; Smith, Q. A.; Nechay, M. R.; Alexandrova, A. N. *Accounts Chem. Res.* **2014**, *47*, 3110-3117.
(7) Dielmann-Gessner, J.; Grossman, M.; Nibali, V. C.; Born, B.; Solomonov, I.; Fields, G. B.; Havenith, M.; Sagi, I. *Proc. Natl. Acad. Sci. U.S.A.* **2014**, *111*, 17857-17862.
(8) Frauenfelder, H.; Chen, G.; Berendzen, J.; Fenimore, P. W.; Jansson, H.; McMahon, B. H.; Stroe, I. R.; Swenson, J.; Young, R. D. *Proc. Natl. Acad. Sci. U.S.A.* **2009**, *106*, 5129-5134.
(9) Xu, Y.; Mayne, L.; Englander, S. W. *Nat. Struct. Biol.* **1998**, *5*, 774-778.
(10) Hammes-Schiffer, S. *Biochemistry* **2013**, *52*, 2012-2020.
(11) Boehr, D. D.; Dyson, H. J.; Wright, P. E. *Chemical Reviews* **2006**, *106*, 3055-3079.
(12) Henzler-Wildman, K.; Kern, D. *Nature* **2007**, *450*, 964-972.
(13) Liuni, P.; Jeganathan, A.; Wilson, D. J. *Angew. Chem. Int. Ed.* **2012**, *51*, 9666 –9669.
(14) Campbell, E.; Kaltenbach, M.; Correy, G. J.; Carr, P. D.; Porebski, B. T.; Livingstone, E. K.; Afriat-Jurnou, L.; Buckle, A. M.; Weik, M.; Hollfelder, F.; Tokuriki, N.; Jackson, C. J. *Nat. Chem. Biol.* **2016**, *12*, 944-+.
(15) Kohen, A.; Klinman, J. P. *J. Am. Chem. Soc.* **2000**, *122*, 10738-10739.
(16) Liang, Z.-X.; Lee, T.; Resing, K. A.; Ahn, N. G.; Klinman, J. P. *Proc. Natl. Acad. Sci. U.S.A.* **2004**, *101*, 9556-9561.
(17) Bhabha, G.; Lee, J.; Ekiert, D. C.; Gam, J.; Wilson, I. A.; Dyson, H. J.; Benkovic, S. J.; Wright, P. E. *Science* **2011**, *332*, 234-238.
(18) Kovermann, M.; Aden, J.; Grundstrom, C.; Sauer-Eriksson, A. E.; Sauer, U. H.; Wolf-Watz, M. *Nat. Commun.* **2015**, *6*.
(19) Holland, D. R.; Tronrud, D. E.; Pley, H. W.; Flaherty, K. M.; Stark, W.; Jansonius, J. N.; McKay, D. B.; Matthews, B. W. *Biochemistry* **1992**, *31*, 11310-11316.
(20) Muller, C. W.; Schlauderer, G. J.; Reinstein, J.; Schulz, G. E. *Structure* **1996**, *4*, 147-156.
(21) Bystroff, C.; Kraut, J. *Biochemistry* **1991**, *30*, 2227-2239.
(22) Larsen, T. M.; Benning, M. M.; Rayment, I.; Reed, G. H. *Biochemistry* **1998**, *37*, 6247-6255.
(23) Joseph, D.; Petsko, G. A.; Karplus, M. *Science* **1990**, *249*, 1425-1428.
(24) Gutteridge, A.; Thornton, J. *FEBS Lett.* **2004**, *567*, 67-73.
(25) Kamerlin, S. C. L.; Warshel, A. *Proc. Natl. Acad. Sci. U.S.A.* **2010**, *107*, E72.
(26) Karplus, M. *Proc. Natl. Acad. Sci. U.S.A.* **2010**, *107*, E71.
(27) Pisliakov, A. V.; Cao, J.; Kamerlin, S. C. L.; Warshel, A. *Proc. Natl. Acad. Sci. U.S.A.* **2009**, *106*, 17359-17364.
(28) Boehr, D. D.; McElheny, D.; Dyson, H. J.; Wright, P. E. *Science* **2006**, *313*, 1638-1642.
(29) Liu, Y.-H.; Konermann, L. *Biochemistry* **2008**, *47*, 6342-6351.

(30) Henzler-Wildman, K. A.; Thai, V.; Lei, M.; Ott, M.; Wolf-Watz, M.; Fenn, T.; Pozharski, E.; Wilson, M. A.; Petsko, G. A.; Karplus, M.; Hubner, C. G.; Kern, D. *Nature* **2007**, *450*, 838-844.
(31) Verkhivker, G. M.; Bouzida, D.; Gehlhaar, D. K.; Rejto, P. A.; Freer, S. T.; Rose, P. W. *Proc. Natl. Acad. Sci. U.S.A.* **2003**, *100*, 5148-5153.
(32) Creighton, T. E. *Proteins*; W. H. Freeman & Co: New York, 1993.
(33) Eliezer, D.; Yao, J.; Dyson, H. J.; Wright, P. E. *Nat. Struct. Biol.* **1998**, *5*, 148-155.
(34) Keppel, T. R.; Howard, B. A.; Weis, D. D. *Biochemistry* **2011**, *50*, 8722-8732.
(35) Wales, T. E.; Engen, J. R. *Mass Spectrom. Rev.* **2006**, *25*, 158-170.
(36) Zhu, M. M.; Rempel, D. L.; Du, Z. H.; Gross, M. L. *J. Am. Chem. Soc.* **2003**, *125*, 5252-5253.
(37) Trelle, M. B.; Hirschberg, D.; Jansson, A.; Ploug, M.; Roepstorff, P.; Andreasen, P. A.; Jørgensen, T. J. D. *Biochemistry* **2012**, *51*, 8256-8266.
(38) Mayne, L.; Paterson, Y.; Cerasoli, D.; Englander, S. W. *Biochemistry* **1992**, *31*, 10678-10685.
(39) Wang, C. Y.; Pawley, N. H.; Nicholson, L. K. *J. Mol. Biol.* **2001**, *313*, 873-887.
(40) Williams, D. C.; Rule, G. S.; Poljak, R. J.; Benjamin, D. C. *J. Mol. Biol.* **1997**, *270*, 751-762.
(41) Massiah, M. A.; Saraswat, V.; Azurmendi, H. F.; Mildvan, A. S. *Biochemistry* **2003**, *42*, 10140-10154.
(42) Emerson, S. D.; Palermo, R.; Liu, C. M.; Tilley, J. W.; Chen, L.; Danho, W.; Madison, V. S.; Greeley, D. N.; Ju, G.; Fry, D. C. *Protein Sci.* **2003**, *12*, 811-822.
(43) Kaltashov, I. A.; Bobst, C. E.; Abzalimov, R. R. *Protein Sci.* **2013**, *22*, 530-544.
(44) Powell, K. D.; Ghaemmaghami, S.; Wang, M. Z.; Ma, L.; Oas, T. G.; Fitzgerald, M. C. *J. Am. Chem. Soc.* **2002**, *124*, 10256-10257.
(45) Percy, A. J.; Rey, M.; Burns, K. M.; Schriemer, D. C. *Anal. Chim. Acta* **2012**, *721*, 7-21.
(46) Bobst, C. E.; Zhang, M.; Kaltashov, I. A. *J. Mol. Biol.* **2009**, *388*, 954-967.
(47) Sowole, M. A.; Alexopoulos, J. A.; Cheng, Y.-Q.; Ortega, J.; Konermann, L. *J. Mol. Biol.* **2013**, *425*, 4508-4519.
(48) Burke, J. E.; Babakhani, A.; Gorfe, A. A.; Kokotos, G.; Li, S.; Woods, V. L.; McCammon, J. A.; Dennis, E. A. *J. Am. Chem. Soc.* **2009**, *131*, 8083-8091.
(49) Shukla, A. K.; Westfield, G. H.; Xiao, K.; Reis, R. I.; Huang, L.-Y.; Tripathi-Shukla, P.; Qian, J.; Li, S.; Blanc, A.; Oleskie, A. N.; Dosey, A. M.; Su, M.; Liang, C.-R., et al. *Nature* **2014**, *512*, 218-222.
(50) Imamura, K.; Tanaka, T. *J. Biochem.* **1972**, *71*, 1043-&.
(51) Liu, V. M.; Vander Heiden, M. G. *Brain Pathol.* **2015**, *25*, 781-783.
(52) Christofk, H. R.; Vander Heiden, M. G.; Harris, M. H.; Ramanathan, A.; Gerszten, R. E.; Wei, R.; Fleming, M. D.; Schreiber, S. L.; Cantley, L. C. *Nature* **2008**, *452*, 230-233.
(53) Anastasiou, D.; Yu, Y. M.; Israelsen, W. J.; Jiang, J. K.; Boxer, M. B.; Hong, B. S.; Tempel, W.; Dimov, S.; Shen, M.; Jha, A.; Yang, H.; Mattaini, K. R.; Metallo, C. M., et al. *Nat. Chem. Biol.* **2012**, *8*, 839-847.
(54) Iqbal, M. A.; Gupta, V.; Gopinath, P.; Mazurek, S.; Bamezai, R. N. K. *FEBS Lett.* **2014**, *588*, 2685-2692.
(55) Dombrauckas, J. D.; Santarsiero, B. D.; Mesecar, A. D. *Biochemistry* **2005**, *44*, 9417-9429.
(56) Jurica, M. S.; Mesecar, A.; Heath, P. J.; Shi, W. X.; Nowak, T.; Stoddard, B. L. *Structure* **1998**, *6*, 195-210.

(57) Prasannan, C. B.; Villar, M. T.; Artigues, A.; Fenton, A. W. *Biochemistry* **2013**, *52*, 1998-2006.
(58) Ou, Y.; Tao, W.; Zhang, Y.; Wu, G.; Yu, S. *Int. J. Biol. Macromol.* **2010**, *47*, 228-232.
(59) Yu, S.; Lee, L. L.-Y.; Lee, J. C. *Biophys. Chem.* **2003**, *103*, 1-11.
(60) Muñoz, E.; Ponce, E. *Comp. Biochem. Physiol. B Biochem. Mol. Biol.* **2003**, *135*, 197-218.
(61) Cheng, X. D.; Friesen, R. H. E.; Lee, J. C. *J. Biol. Chem.* **1996**, *271*, 6313-6321.
(62) Consler, T. G.; Jennewein, M. J.; Cai, G. Z.; Lee, J. C. *Biochemistry* **1992**, *31*, 7870-7878.
(63) Oria-Hernández, J.; Cabrera, N.; Pérez-Montfort, R.; Ramírez-Silva, L. *Journal of Biological Chemistry* **2005**, *280*, 37924-37929.
(64) Lodato, D. T.; Reed, G. H. *Biochemistry* **1987**, *26*, 2243-2250.
(65) Long, D.; Marshall, C. B.; Bouvignies, G.; Mazhab-Jafari, M. T.; Smith, M. J.; Ikura, M.; Kay, L. E. *Angew. Chem. Int. Ed.* **2013**, *52*, 10771-10774.
(66) Rand, K. D.; Zehl, M.; Jorgensen, T. J. D. *Acc. Chem. Res.* **2014**, *47*, 3018-3027.
(67) Marciano, D. P.; Dharmarajan, V.; Griffin, P. R. *Curr. Op. Struct. Biol.* **2014**, *28*, 105-111.
(68) Vahidi, S.; Bi, Y. M.; Dunn, S. D.; Konermann, L. *Proc. Natl. Acad. Sci. U.S.A.* **2016**, *113*, 2412-2417.
(69) Englander, S. W.; Mayne, L.; Krishna, M. M. G. *Quart. Rev. Biophys.* **2007**, *40*, 287-326.
(70) Skinner, J. J.; Lim, W. K.; Bedard, S.; Black, B. E.; Englander, S. W. *Protein Sci.* **2012**, *21*, 996-1005.
(71) Deredge, D.; Li, J. W.; Johnson, K. A.; Wintrode, P. L. *J. Biol. Chem.* **2016**, *291*, 10078-10088.
(72) Oyeyemi, O. A.; Sours, K. M.; Lee, T.; Kohen, A.; Resing, K. A.; Ahn, N. G.; Klinman, J. P. *Biochemistry* **2011**, *50*, 8251-8260.
(73) Espada, A.; Broughton, H.; Jones, S.; Chalmers, M. J.; Dodge, J. A. *J. Med. Chem.* **2016**, *59*, 2255-2260.
(74) Underbakke, E. S.; Iavarone, A. T.; Chalmers, M. J.; Pascal, B. D.; Novick, S.; Griffin, P. R.; Marletta, M. A. *Structure* **2014**, *22*, 602-611.
(75) Donovan, K. A.; Zhu, S. L.; Liuni, P.; Peng, F.; Kessans, S. A.; Wilson, D. J. *J. Biol Chem.* **2016**, *291*, 9244-9256.
(76) Prasannan, C. B.; Artigues, A.; Fenton, A. W. *Anal. Bioanal. Chem.* **2011**, *401*, 1083-1086.
(77) Wolf-Watz, M.; Thai, V.; Henzler-Wildman, K.; Hadjipavlou, G.; Eisenmesser, E. Z.; Kern, D. *Nat. Struct. Mol. Biol.* **2004**, *11*, 945-949.
(78) Wood, T. *Biochem. Biophys. Res. Comm.* **1968**, *31*, 779-785.
(79) Gallo, A. A.; Sable, H. Z. *Biochim. Biophys. Acta* **1973**, *302*, 443-456.
(80) Anderson, J. S.; Hernandez, G.; LeMaster, D. M. *Biophys. Chem.* **2013**, *171*, 63-75.
(81) Shaw, B. F.; Arthanari, H.; Narovlyansky, M.; Durazo, A.; Frueh, D. P.; Pollastri, M. P.; Lee, A.; Bilgicer, B.; Gygi, S. P.; Wagner, G.; Whitesides, G. M. *J. Am. Chem. Soc.* **2010**, *132*, 17411-17425.
(82) Bai, Y.; Milne, J. S.; Mayne, L.; Englander, S. W. *Proteins: Struct., Funct., Genet.* **1993**, *17*, 75-86.
(83) Xiao, Y.; Shaw, G. S.; Konermann, L. *J. Am. Chem. Soc.* **2017**, *139*, 11460-11470.
(84) Nemirovskiy, O.; Giblin, D. E.; Gross, M. L. *J. Am. Soc. Mass Spectrom.* **1999**, *10*, 711-718.
(85) Skinner, J. J.; Lim, W. K.; Bedard, S.; Black, B. E.; Englander, S. W. *Protein Sci.* **2012**, *21*, 987-995.
(86) Boehr, D. D.; Nussinov, R.; Wright, P. E. *Nat. Chem. Biol.* **2009**, *5*, 789-796.
(87) Koshland, D. E., Jr. *Proc. Natl. Acad. Sci. U.S.A.* **1958**, *44*, 98-104.

(88) Seeholzer, S. H.; Jaworowski, A.; Rose, I. A. *Biochemistry* **1991**, *30*, 727-732.
(89) Zeymer, C.; Werbeck, N. D.; Zimmermann, S.; Reinstein, J.; Hansen, D. F. *Angew. Chem.-Int. Edit.* **2016**, *55*, 11533-11537.

Figure Captions

Figure 1. Crystal structure of *r*M1-PK (pdb code 1A49).[22] (a) Complete tetramer. Each subunit consists of four domains; N (cyan, residues 12-42), A (43-115 and 219-387, red), B (116-218, green); C (388-530, blue). The active site is located in the cleft between domains A and B. (b) Catalytic sequence, where the *r*M1-PK enzyme is denoted as "E". Dots indicate noncovalent protein-ligand contacts. Panels (c) - (e) illustrate active site closure for one of the subunits via rotation of domain B after Mg-ATP (dark gray) and oxalate (magenta) binding. K^+ and Mg^{2+} are shown in orange and yellow, respectively. (c) Closed state in the presence of Mg-ATP and oxalate. (d) Semi-closed state in the presence of Mg-ATP and oxalate. (e) Open state in the presence of oxalate, without nucleotide.

Figure 2. (a) Locations of peptides 110-123, 292-298, and 365-374 in the *r*M1-PK active site.[22] Unprocessed mass spectra of segment 365-374 after 1 min of HDX are shown for the resting state (b), and under working conditions with substrate turnover (c). Vertical dashed lines in panels b, c represent isotope distribution centroids.

Figure 3. HDX kinetic plots for selected *r*M1-PK peptides (110-123, 292-298, and 365-374, as noted along the top) under different conditions. For the locations of these peptides within the enzyme structure, see Figure 2a. Each panel contains data for the resting state (with K^+ and Mg^{2+} bound, gray asterisks). (a-c) Comparison of resting state and working state. Note that catalytic turnover takes place only up to t = 1 min. (d-f) Effects of substrate (PEP and Mg-ADP) binding. (g-i) Effects of pseudo-product (oxalate) and Mg-ATP binding. (j-l) Effects of metal depletion, and after addition of only K^+ or Mg^{2+} back into the solution.

Figure 4. HDX difference plots for t = 1 min relative to the resting state, i.e., [%D(current state) - %D(resting state)], mapped to the crystal structures of one *r*M1-PK subunit. The "current state" is indicated in each panel. Blue represents regions with less deuteration than the resting state; red indicates more deuteration than the resting state (see legend, top right). The ordering of experimental conditions is as in Figure 3. Regions not covered by the peptic mapping are indicated in dark grey. The ligands shown represent the available crystal structures[22] and do not always exactly match to the ligands present in the corresponding HDX/MS experiments.

Figure 1

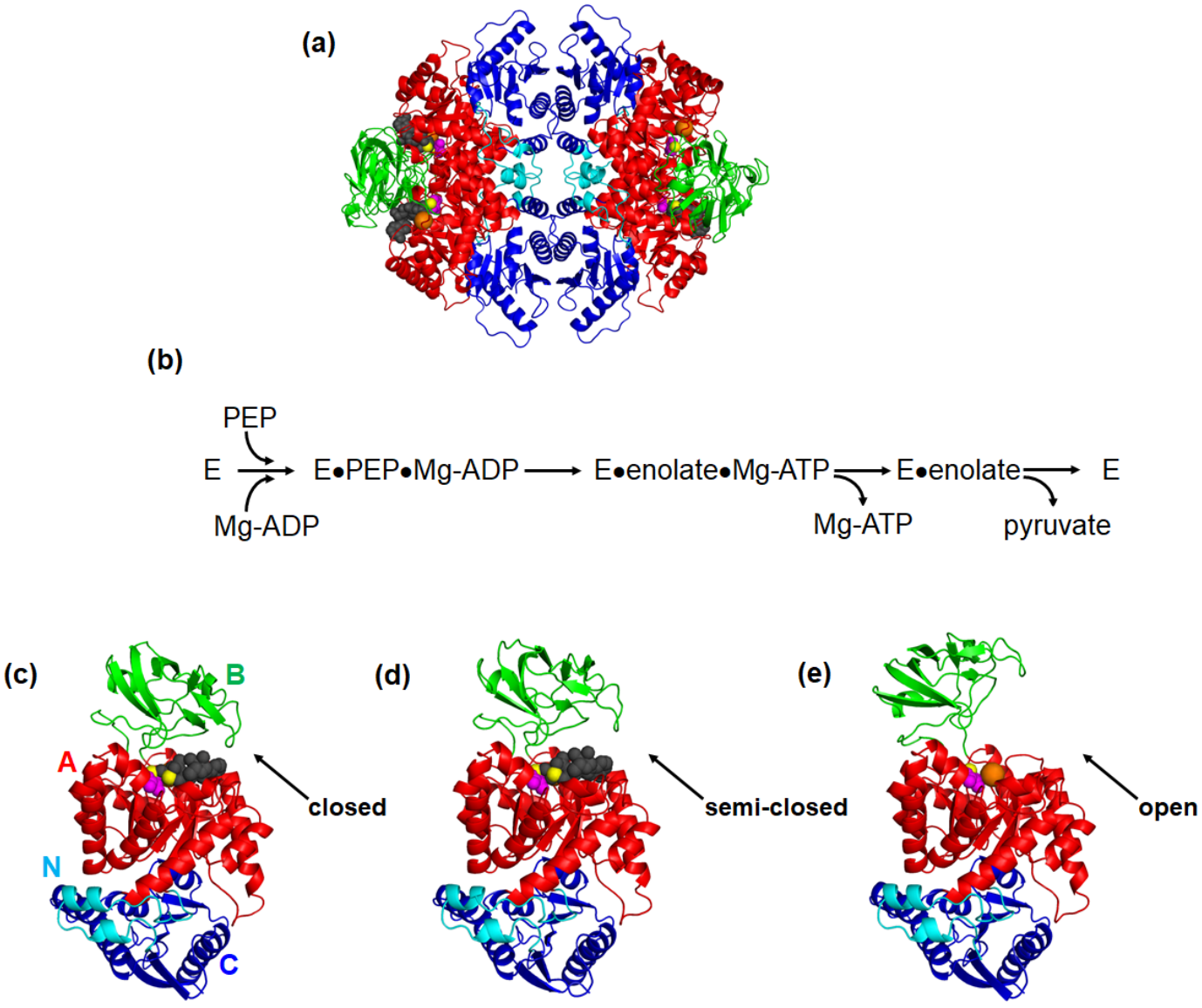
(a)
(b)
PEP
E
E•PEP•Mg-ADP
E•enolate•Mg-ATP
E•enolate
E
Mg-ADP
Mg-ATP
pyruvate
(c)
B
A
N
C
closed
(d)
semi-closed
(e)
open

Figure 2

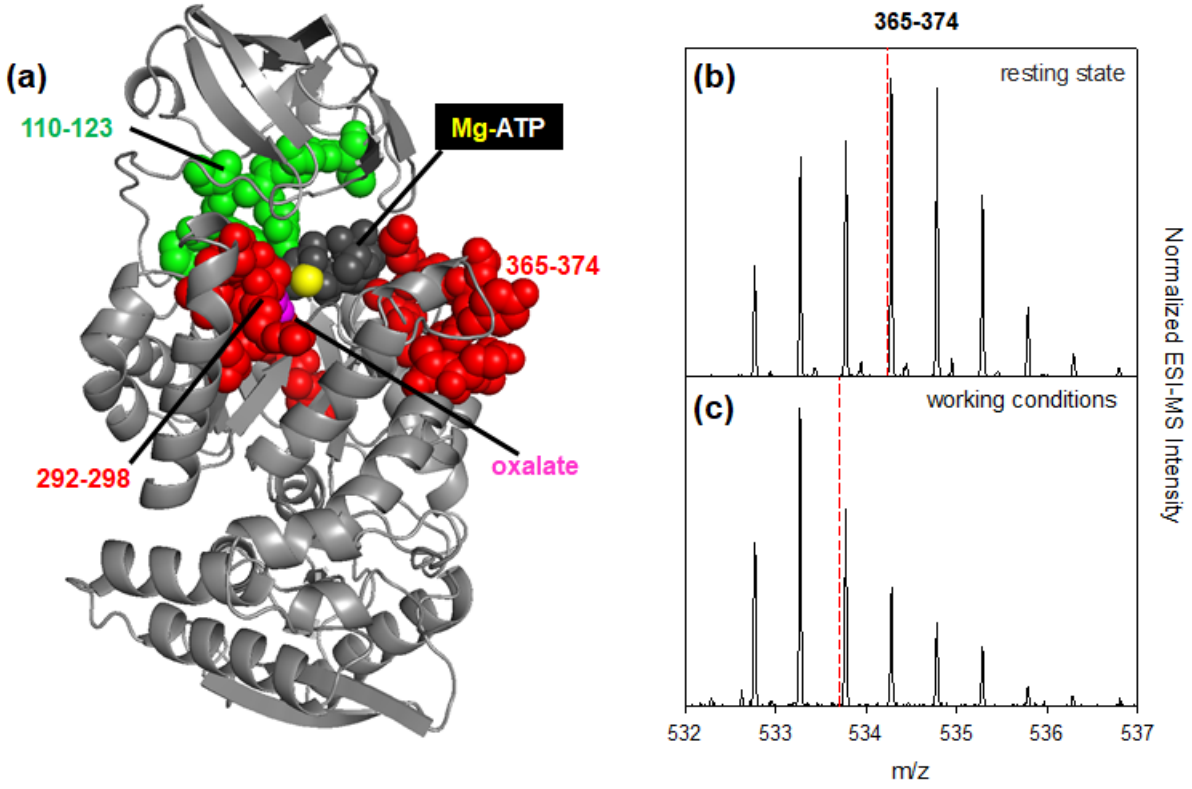
(a)
110-123
Mg-ATP
365-374
292-298
oxalate
365-374
(b)
resting state
(c)
working conditions
Normalized ESI-MS Intensity
532
533
534
535
536
537
m/z

Figure 3

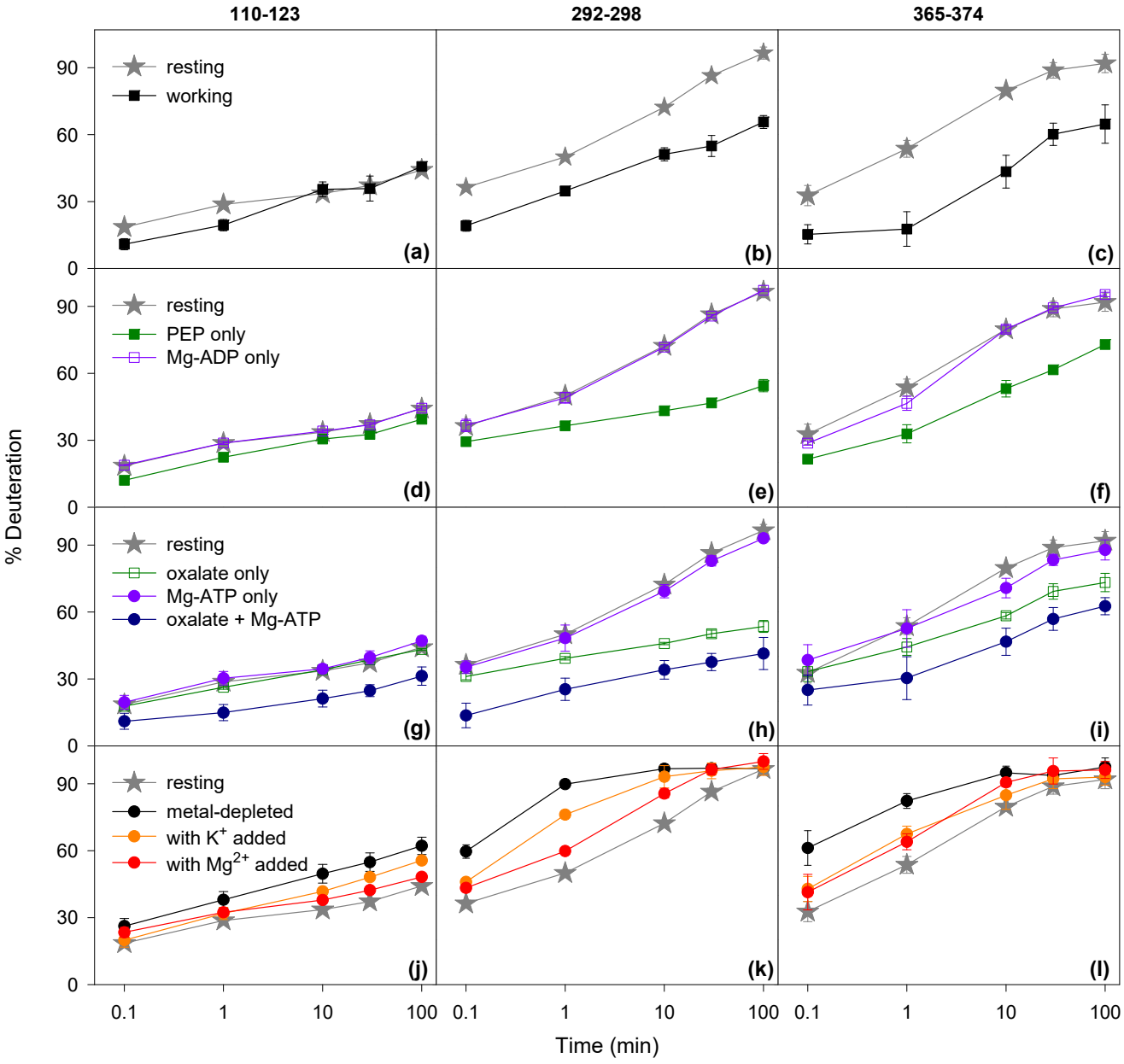
110-123
292-298
365-374
resting
working
PEP only
Mg-ADP only
oxalate only
Mg-ATP only
oxalate + Mg-ATP
metal-depleted
with K+ added
with Mg2+ added
(a)
(b)
(c)
(d)
(e)
(f)
(g)
(h)
(i)
(j)
(k)
(l)
% Deuteration
Time (min)
0
30
60
90
0.1
1
10
100

Figure 4

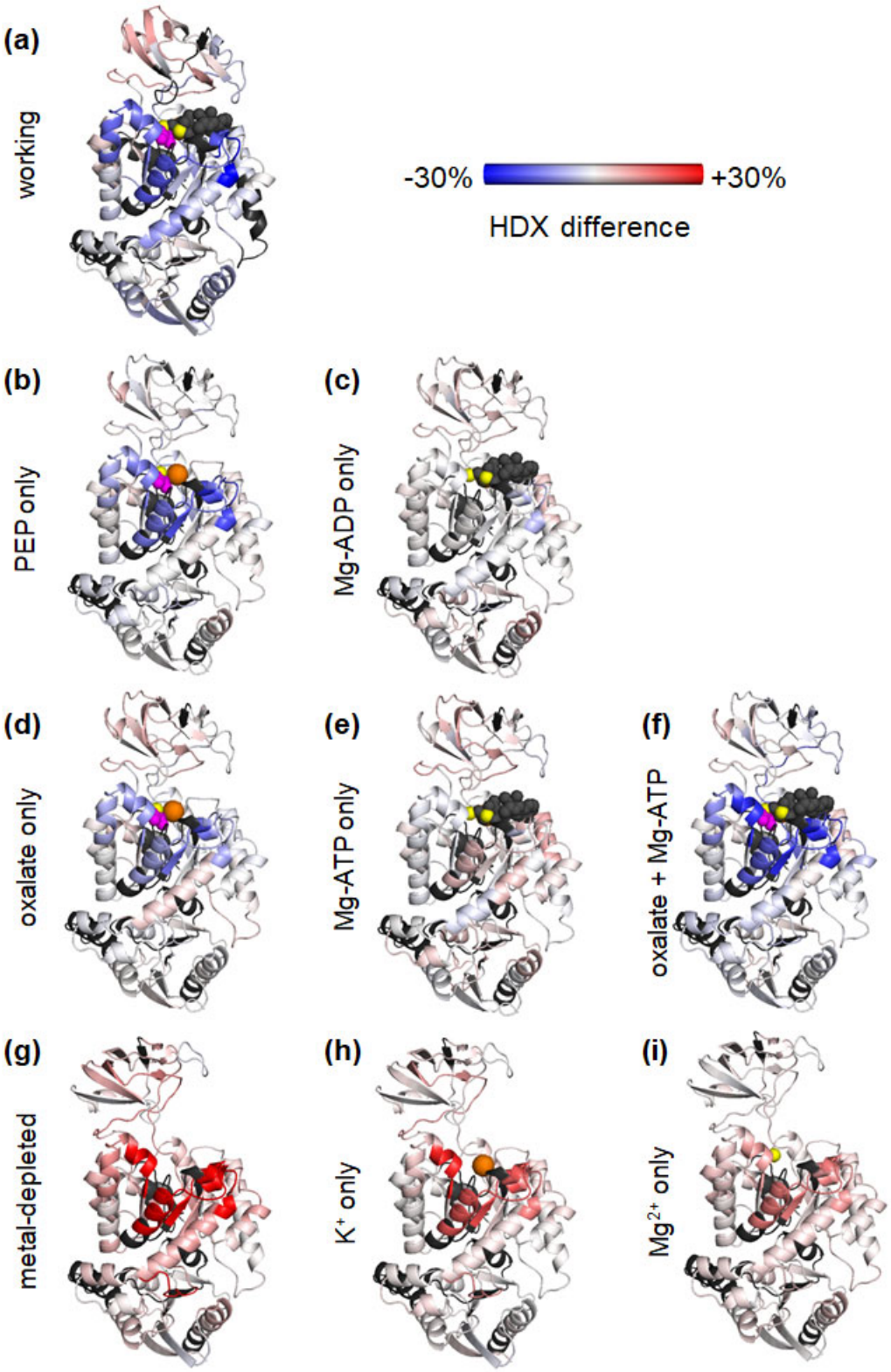
(a)
working
-30%
+30%
HDX difference
(b)
PEP only
(c)
Mg-ADP only
(d)
oxalate only
(e)
Mg-ATP only
(f)
oxalate + Mg-ATP
(g)
metal-depleted
(h)
K+ only
(i)
Mg2+ only

For TOC Only

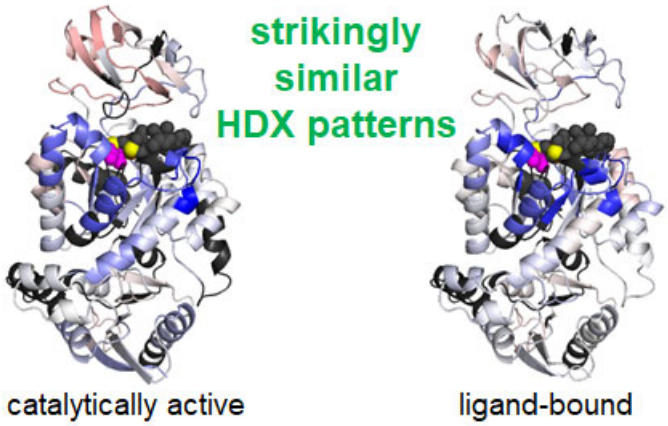
strikingly
similar
HDX patterns
catalytically active
ligand-bound